

The **parsec-scale jets**
of the **SS 433 microquasar**
seen in **very-high-energy γ -rays** with **H.E.S.S.**

Michelle Tsirou^o

&

Laura Olivera-Nieto*, Brian Reville^o, Jim Hinton^o,
on behalf of the **H.E.S.S. collaboration**

“Matter and the Universe” Days

Hamburg, Germany

12 . 12. 2024

* : first author
o : corresponding authors



The curious case of SS 433 : an extraordinary microquasar



artist's rendering @ Science Communication Lab

“Manatee nebula” :
W 50 / SNR G039.7-02.0
Supernova remnant
seen in **radio**

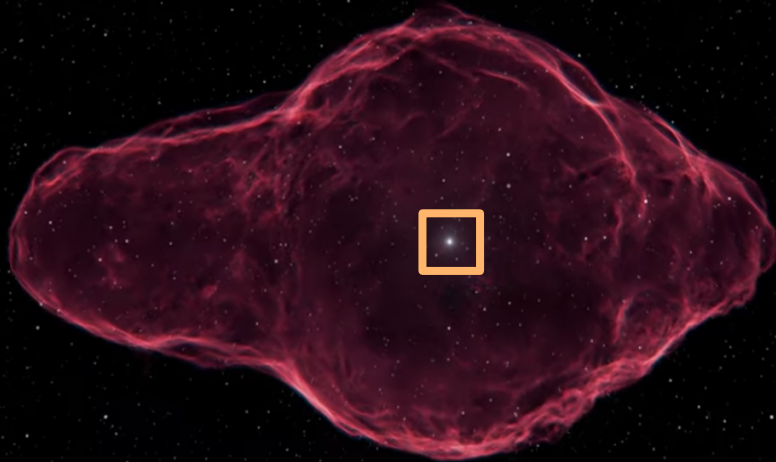
~ age : [10 -100] kyr



Credit : H.E.S.S. / MPIK

[YT link](#) 02α / 12

The curious case of SS 433 : an extraordinary microquasar



artist's rendering @ Science Communication Lab

At the "centre"
of W 50

d ~ 5.5kpc from us



Credit : H.E.S.S. / MPIK

[YT link](#) 02β / 12

The curious case of SS 433 : an extraordinary microquasar

black hole

type A supergiant

artist's impression @ Science Communication Lab

Binary system :
Compact object
(likely BH $\sim 10 M_{\odot}$)
orbiting its
companion star
with a period
 ~ 13 days



Credit : H.E.S.S. / MPIK

[YT link](#) 02γ / 12

The curious case of SS 433 : an extraordinary microquasar

black hole

type A supergiant

artist's impression @ Science Communication Lab

- high accretion rate
- jet launching

What about the electromagnetic beams?



Credit : H.E.S.S. / MPIA

[YT link](#) 028 / 12

The curious case of SS 433 : an extraordinary microquasar



artist's rendering @ Science Communication Lab

“Inner jets” :
Collimated beams
precessing with
 $\theta \sim 20^\circ$
period ~ 162 days
Seen in **radio**
 $\rightarrow v_{\text{jet}} \sim 0.26c$



Credit : H.E.S.S. / MPIK

[YT link](#) 02ε / 12

The curious case of SS 433 : an extraordinary microquasar

“Inner jets” :
What about beyond
0.1 pc?

→ emission too dim



Credit : H.E.S.S. / MPIK

[YT link](#) 027 / 12

artist's rendering @ Science Communication Lab

The curious case of SS 433 : an extraordinary microquasar

“Outer jets” :
Bright **X-ray** emission

re-collimated
outflow
w/o detected
motion



Credit : H.E.S.S. / MPIK

[YT link](#) 02η / 12

25 parsecs

artist's impression @ Science Communication Lab

The curious case of SS 433 : an extraordinary microquasar

“Outer jets” :

Terminating ~ 100 pc
from the BH

UL v_{jet} at the edge
 $\sim 0.023c$



Credit : H.E.S.S. / MPIK

[YT link](#) 020 / 12

75 parsecs

artist's impression @ Science Communication Lab

The curious case of SS 433 : an extraordinary microquasar

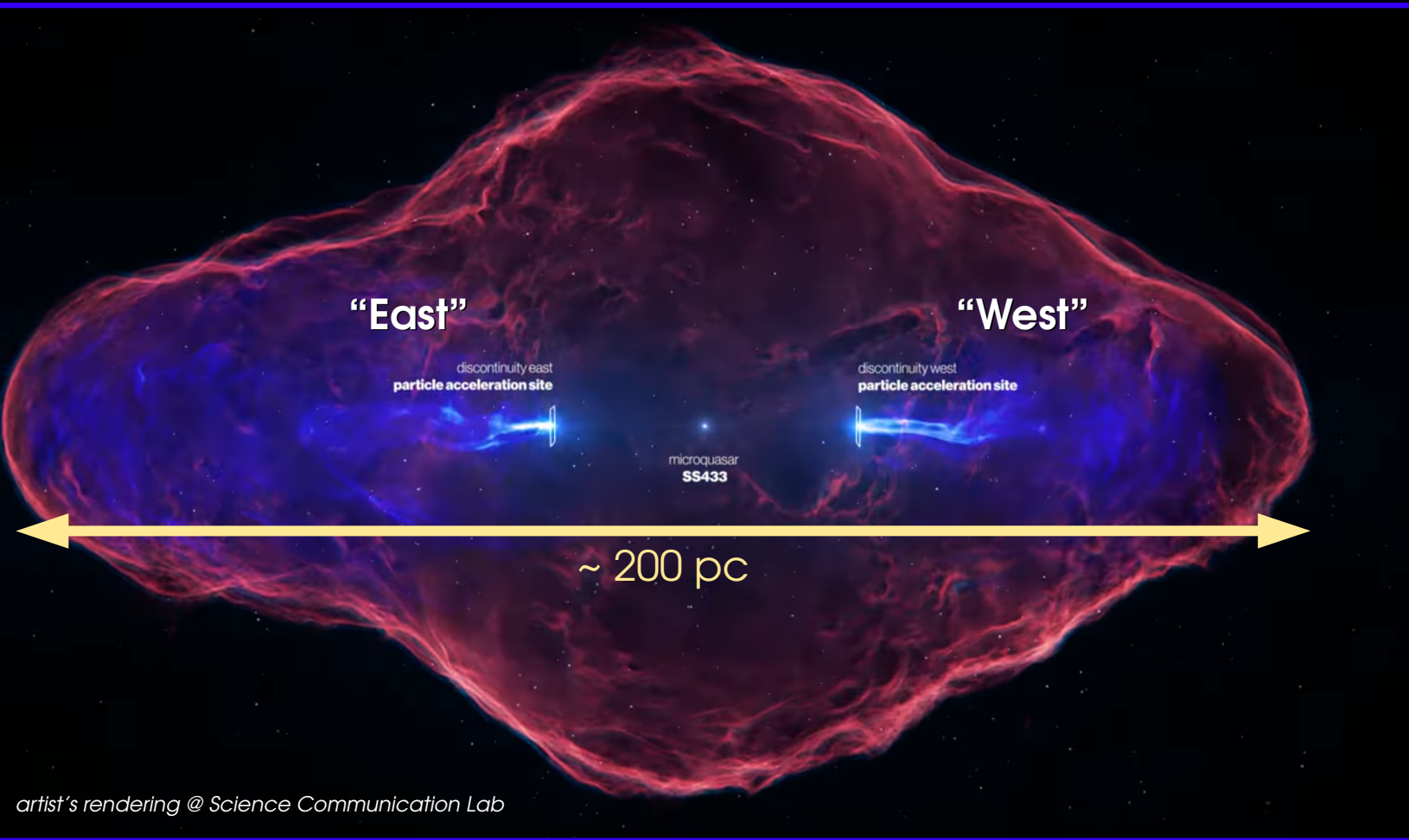
“Outer jets” :

Parsec-scale
re-collimated jets
of e^-/e^+



Credit : H.E.S.S. / MPIK

[YT link](#) 02 / 12



artist's rendering @ Science Communication Lab

Claims of observed γ -ray emission : no consensus!

High-energies (MeV-GeV)

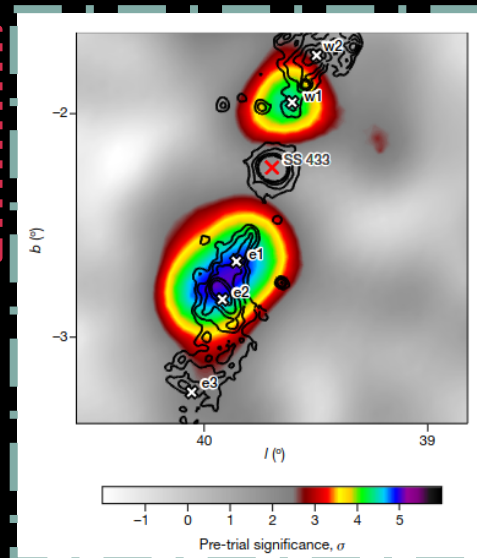
Very-high-energies (TeV)

→ Where is the γ -ray emission coming from?
 → What are its **characteristics**?

Fang et al, 2020, "hotspots"

(100 MeV - 300 GeV)

(Fermi-LAT + HAWC)

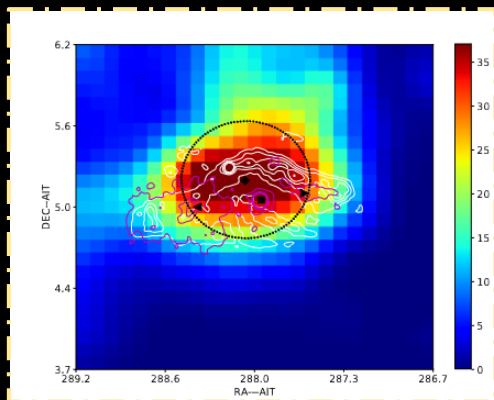


HAWC collaboration, 2018
 (2 "hotspots" at 20 TeV)

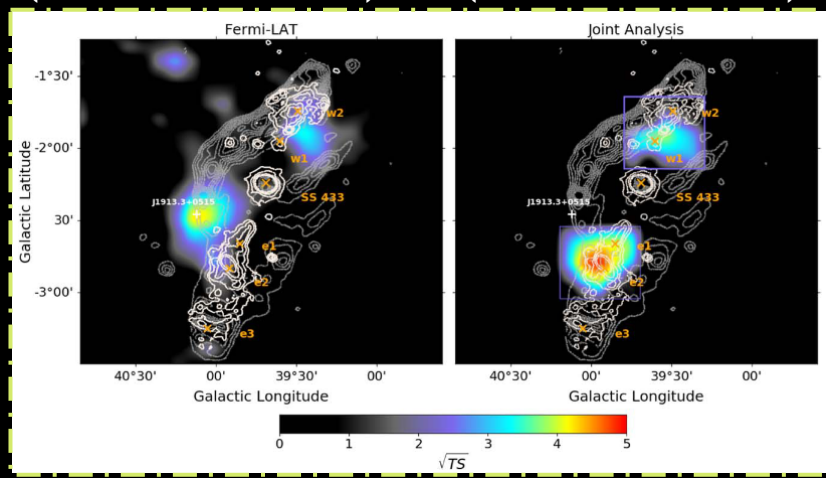
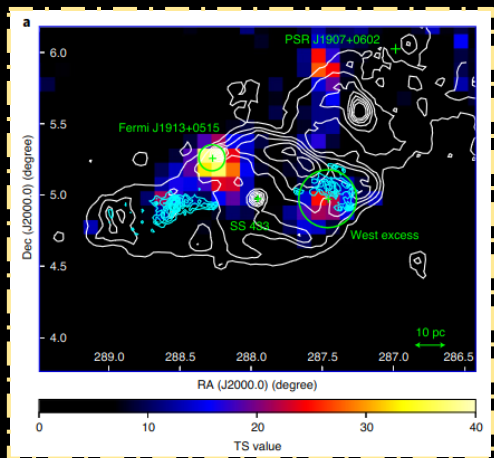
+ many many more
 also interesting studies
 throughout the years!

03 / 12

Sun et al, 2019
 (> 500 MeV)



Li et al, 2020
 (100 MeV - 300 GeV)
 OFF phase PSR J1907+0602



High Energy Stereoscopic System

- Archival observations (centered on HESS J1908+063, source at the north-west FoV)
- Observation campaign in 2020-2021 to homogenise the exposure
→ ~ > **200 hours of H.E.S.S. data**
- Use of a new analysis technique, with **optimisation for higher E and “faint” emission** :
use the large CT to **improve background rejection!**
 - [Olivera-Nieto et al, EPJC 81 1101 \(2021\)](#) Muons as a tool for bkg rejection in IACTs
 - + [Olivera-Nieto et al, EPJC 82 1118 \(2022\)](#) Algorithm for Background Rejection using Image Residuals (ABRIR)

System of (4 medium-sized + 1 large)
Imaging Atmospheric Cherenkov Telescopes
→ ~0.01 TeV up to ~100 TeV



H.E.S.S. site at Khomas Highland, Namibia

Detection of **extended VHE γ -ray emission**
correlating spatially with the **outer jets**

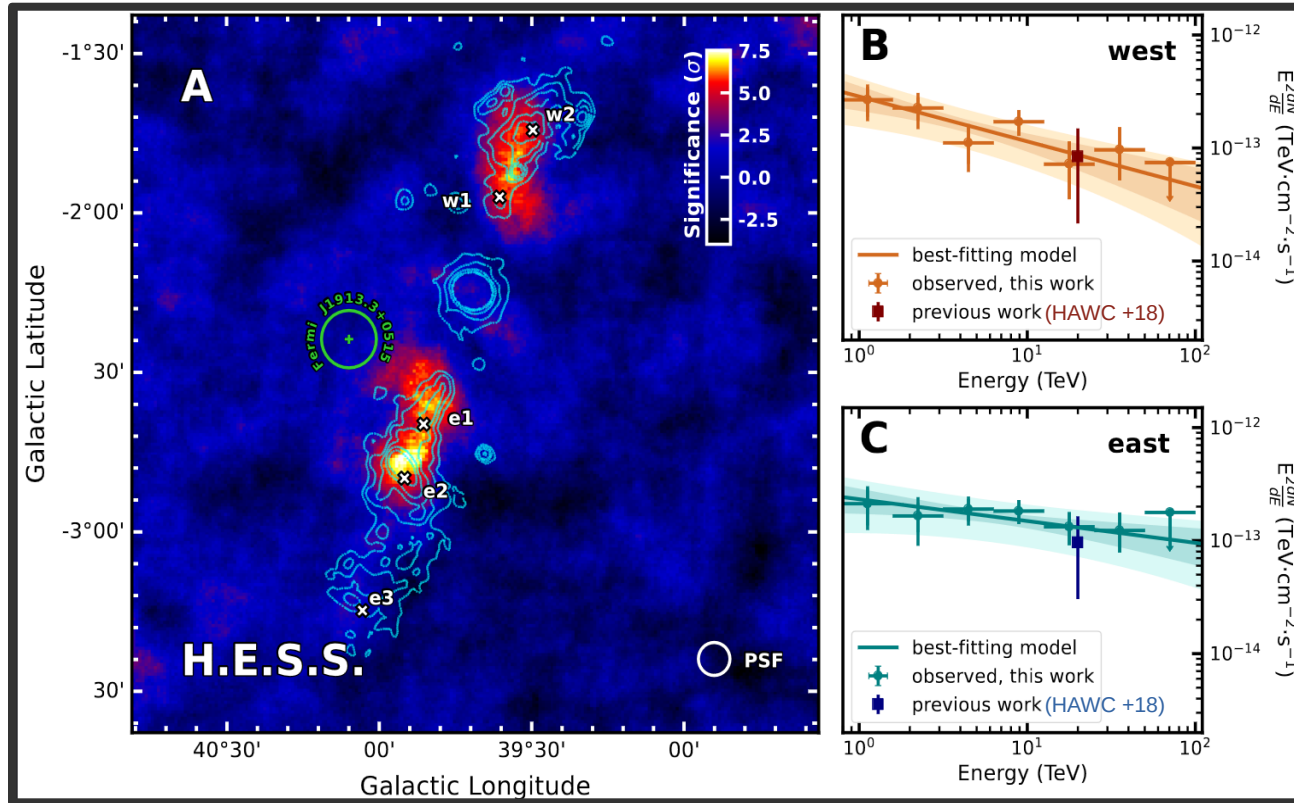
→ spectro-morphological analysis
Science, 383, 6681, pp. 402-406 (2024)
H.E.S.S. Collaboration

Detection of the SS 433 system with H.E.S.S. : first time with an IACT array

Only $< 1.5\sigma$ preference for spectral steepening
 → confirming hard spectra for both!

No TeV
 emission from
 Fermi
 J1913+0515

DOI: 10.1126/science.adi2048



West :

- **6.8 σ** detection
- Gaussian_{asym} :
 - 3.5 σ w.r.t a Gaussian_{sym}
 - 4.7 σ w.r.t a point-like description
- ϕ spectral index :
2.40 \pm 0.15_{stat} \pm 0.13_{syst}

East :

- **7.8 σ** detection
- Gaussian_{asym} :
 - 5.8 σ w.r.t a Gaussian_{sym}
 - 7.8 σ w.r.t a point-like description
- ϕ spectral index :
2.19 \pm 0.12_{stat} \pm 0.12_{syst}
 05 α / 12

Overlaid ROSAT X-ray contours for ref

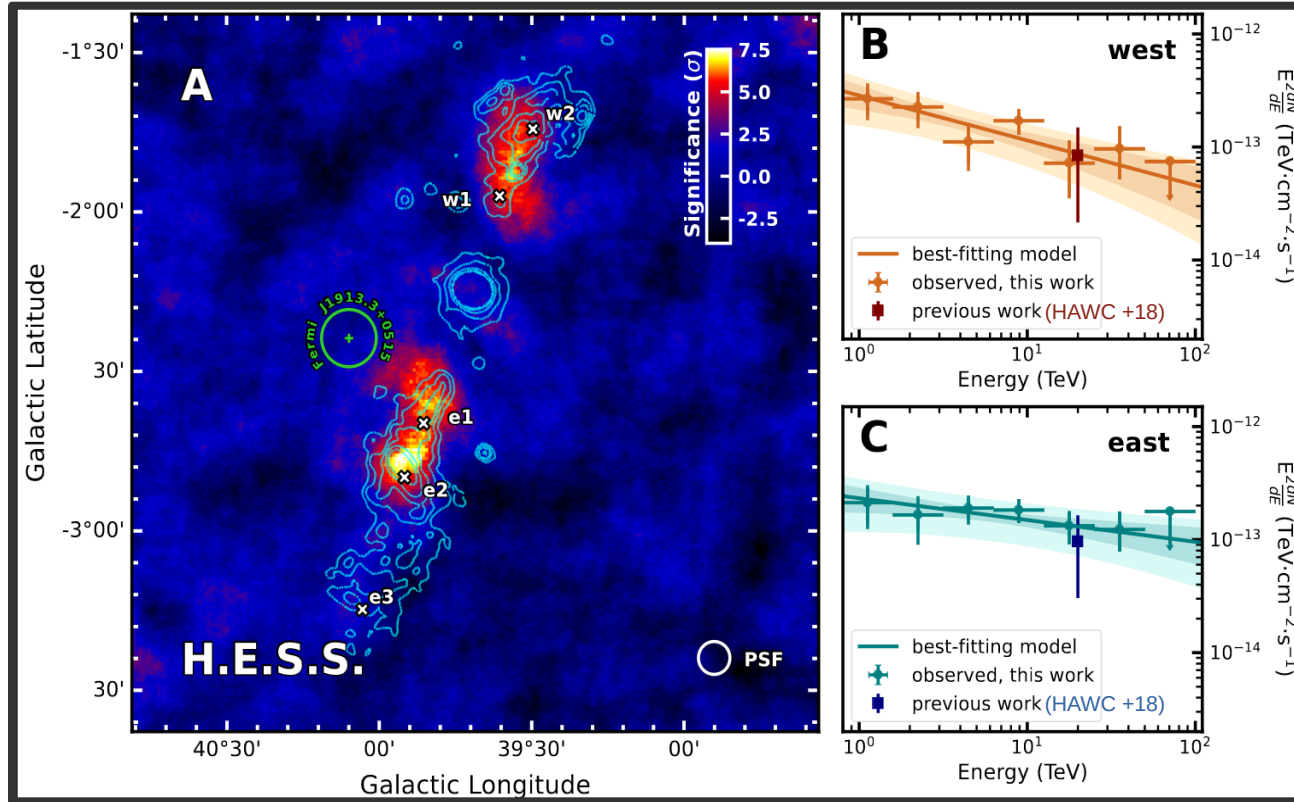
Detection of the SS 433 system with H.E.S.S. : the gist

West :

→ confirming hard spectra for both!

No TeV
emission from
Fermi
J1913+0515
seen by
H.E.S.S.

DOI: 10.1126/science.adf2048



size
~

13 pc x 5 pc

- ϕ spectral index :
 $2.40 \pm 0.15_{\text{stat}} \pm 0.13_{\text{syst}}$

East :

size
~

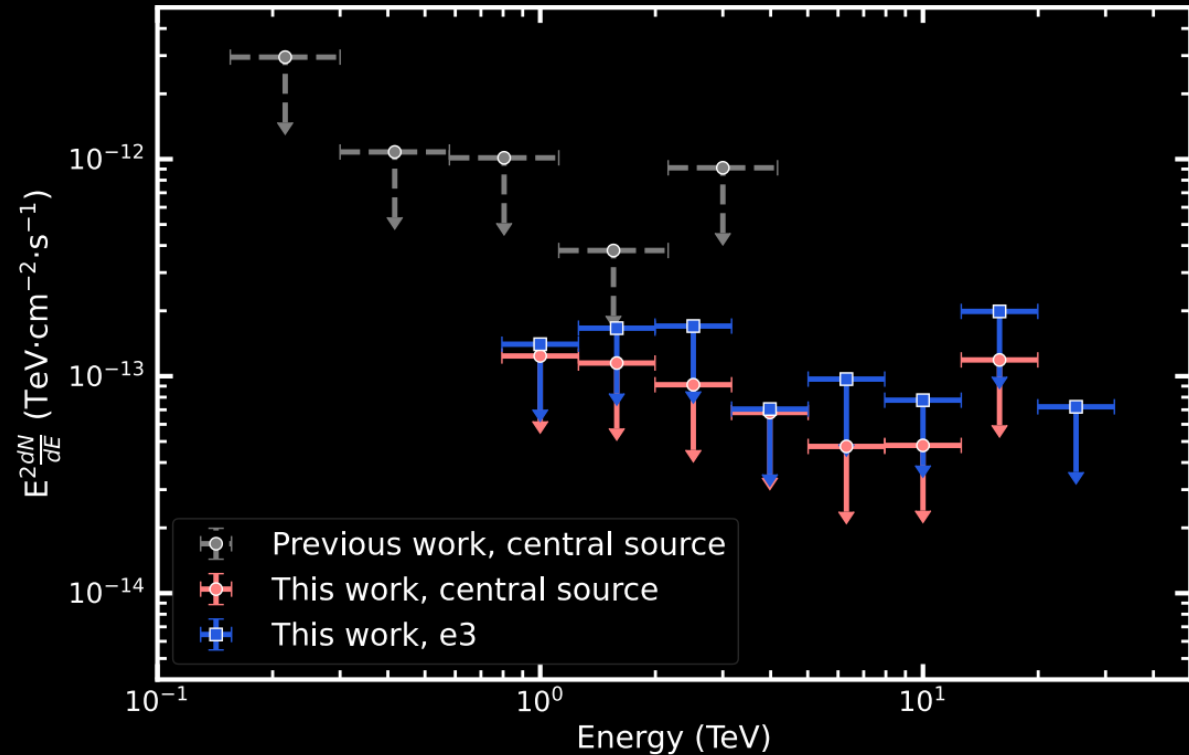
20 pc x 4 pc

- ϕ spectral index :
 $2.19 \pm 0.12_{\text{stat}} \pm 0.12_{\text{syst}}$

Overlaid ROSAT X-ray contours for ref

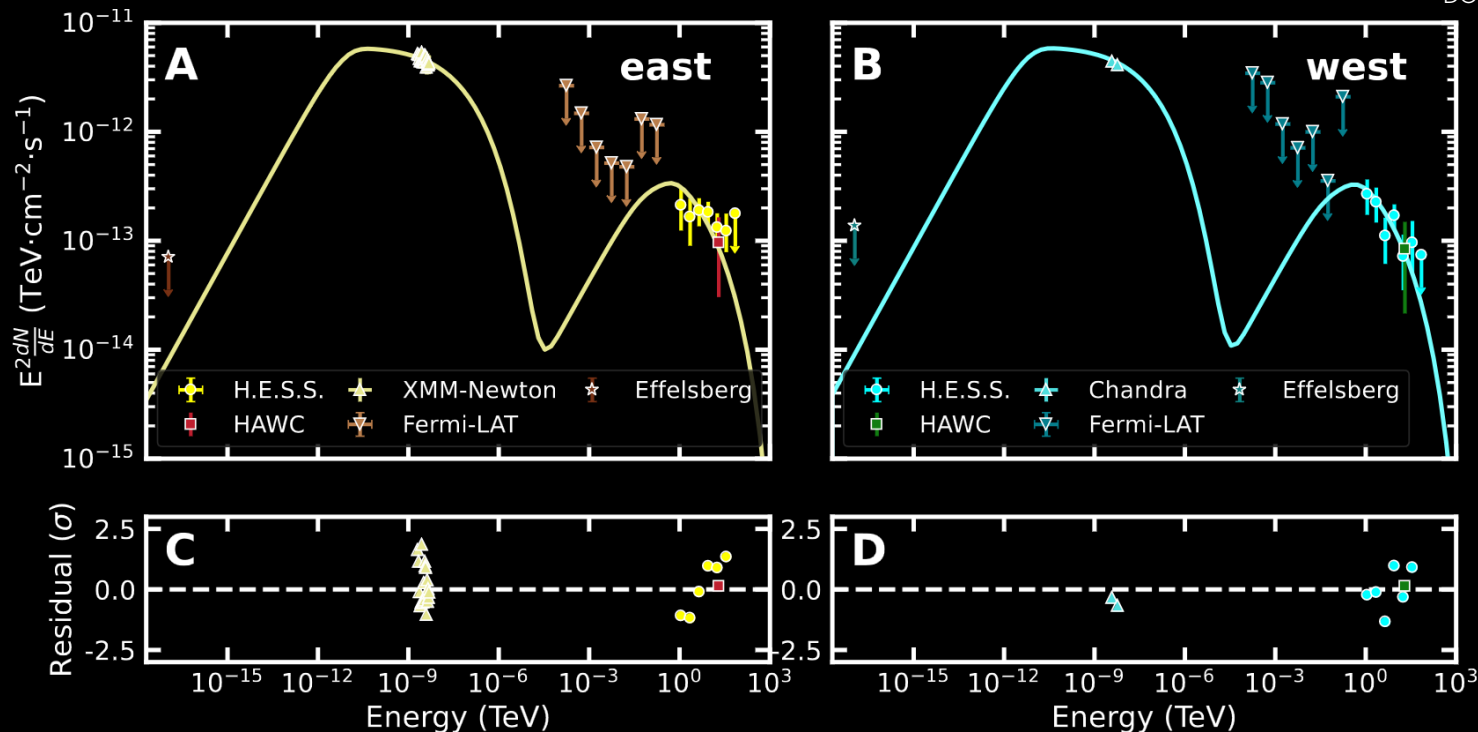
- x No periodic variability seen by H.E.S.S.

 - x No $> 5\sigma$ emission
 - from the central binary
 - nor
 - from the far eastern region of the X-ray jet (e3)
- only thermal radiation seen in X-rays



Leptonic scenario : synchrotron and inverse Compton scattering

DOI: 10.1126/science.adi2048

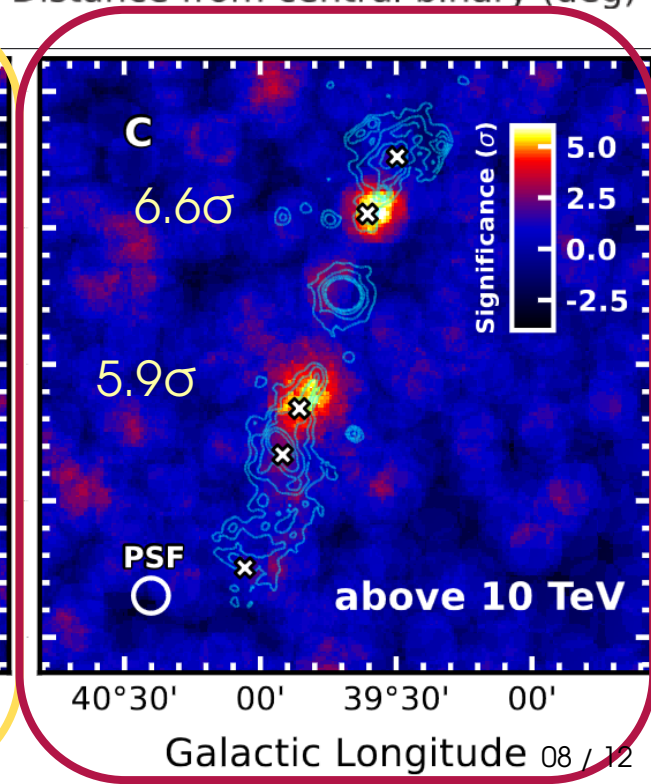
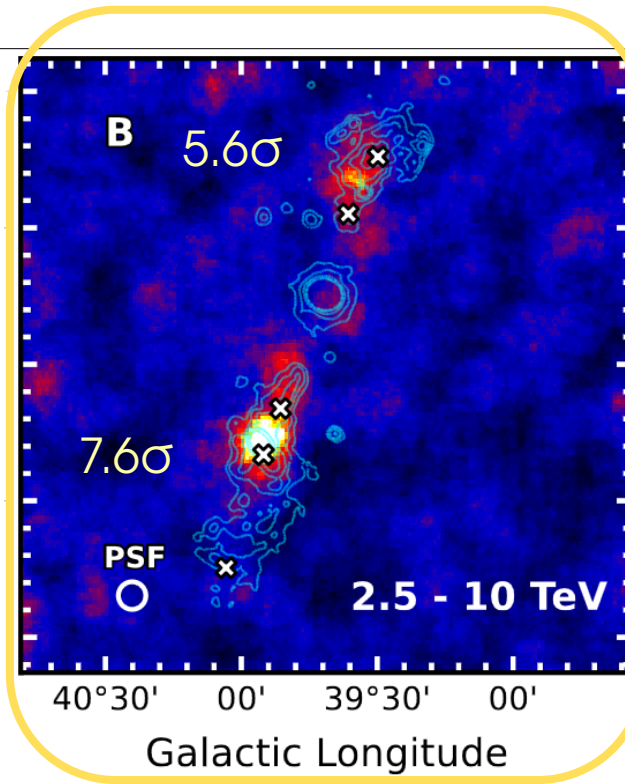
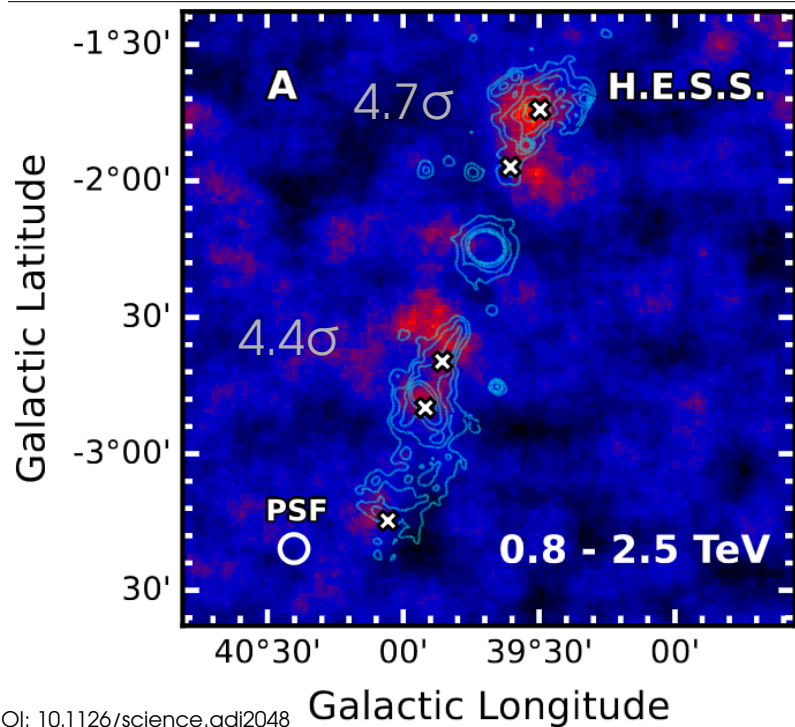
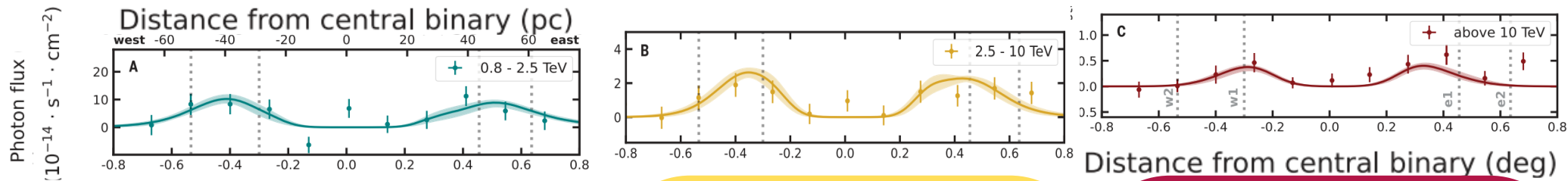


$\Gamma_e = (2s_{\text{SYN}} - 1)$
 ECPL shape
 $E_{\text{dot,tot}} \sim 10^{39} \text{ erg} \cdot \text{s}^{-1}$
 Mean strength in 1-zone

	east	west
Γ_e	2	2
$E_{\text{cut}} \text{ (TeV)}$	>200	
α	$(1.287 \pm 0.029) \cdot 10^{-3}$	
$B \text{ (}\mu\text{G)}$	19.5 ± 2.7	21.1 ± 1.8

Electron index
 Energy cut-off
 % jet kinetic power
 B-field

Energy-dependent morphology



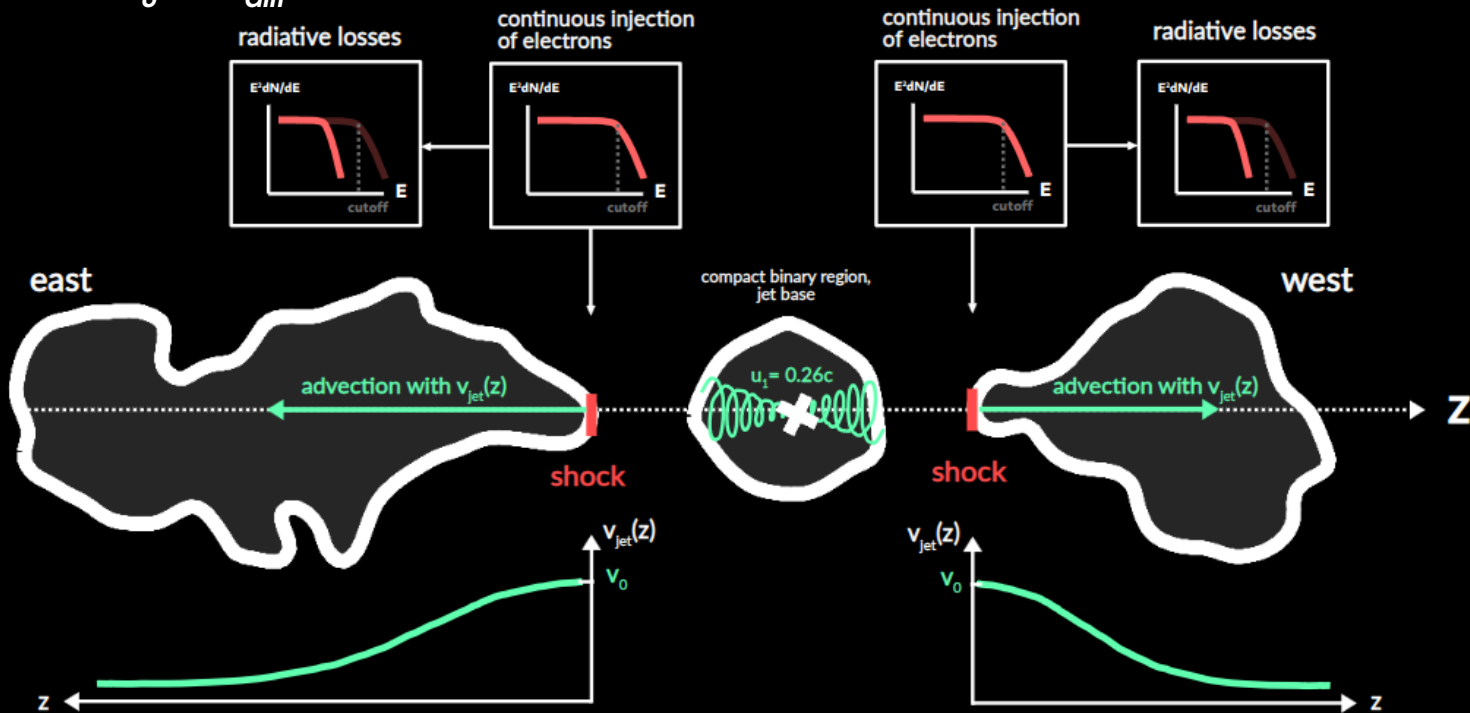
DOI: 10.1126/science.adi2048

08 / 12

Inference of a strong shock at ~ 30 pc

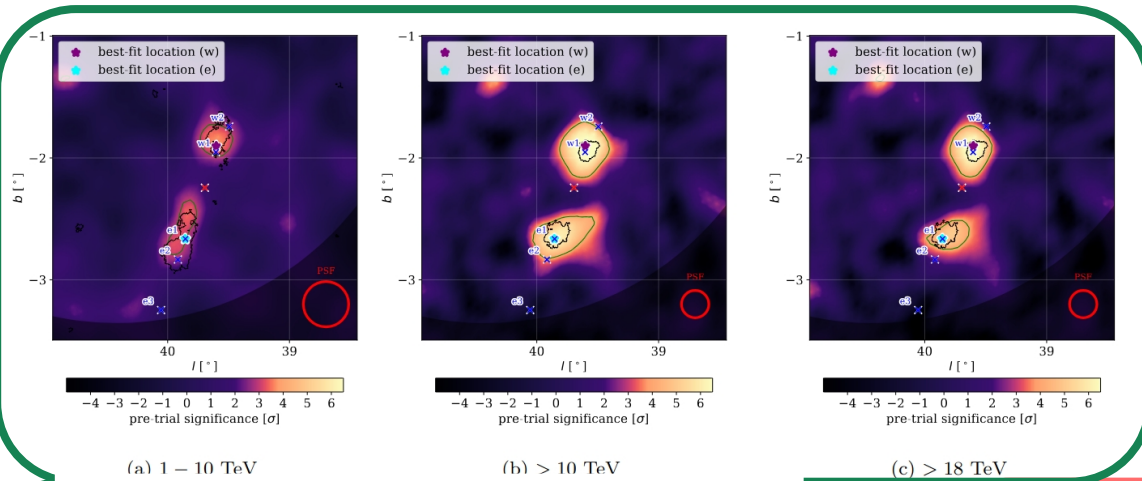
1D MC transport "simulation" along jet axis yielding an output $n_e(E, z)$:

- e^- spectrum, B : [fixed to best-fit MWL SED model of the lobes]
- $v(z) [= v_0 \Lambda(z)]$: [with Λ based on the width of the X-ray jet opening]
- v_0 & D_{diff} **thawed parameters**



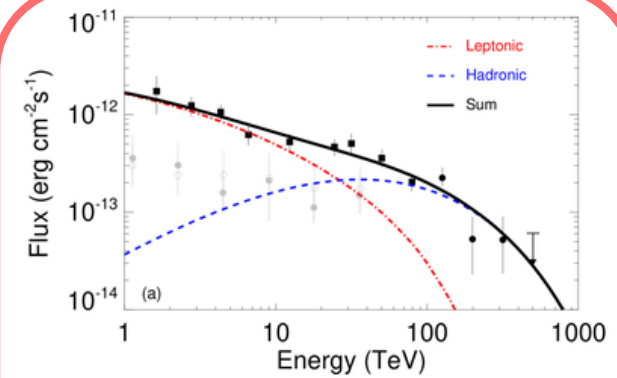
- e^- injected at $z=0$ up to 10 kyr
- advected by $z_{adv} = v_{jet}(z) t$
- scaled with $r = (2 D_{diff} t)^{1/2}$
- cooled

Very-high-energies (>TeV)



Ultra-high-energies (>100 TeV)

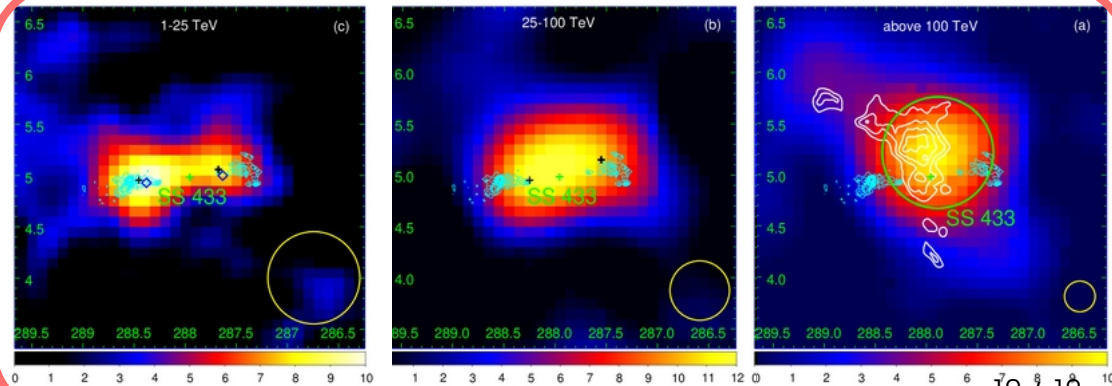
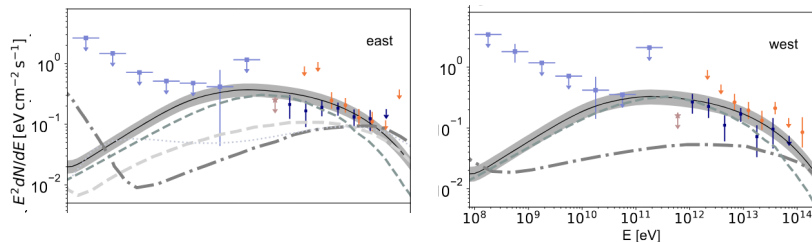
Exciting results, despite the limited morphology resolution !



LHAASO collaboration, 2024

- Sudo+ (2020)
- Kimura+ (2020)
- Reynos & Carilli (2019)
- H.E.S.S.+(2024)
- Fang et al (2020)
- Fermi-LAT (2020)
- VERITAS 99% UL (2017)
- HAWC (this work)
- HESS (2024)

HAWC collaboration, 2024
using 2565 days of data



- SS 433 : still a lot of unsolved questions...
- No detection < 1 TeV of any significant emission from SS 433 or other HE hotspots in the FoV
- No detection of the central binary
- No significant variability
- **Significant detection of extended emission for the east and west parsec-scale jets**
- **Energy-dependent** morphology :
shift of VHE centroid **towards the outer jet base** as a function of E
- Leptonic dominant process to explain the emission in the TeV range : IC scattering on target φ fields
- Inference of a CD/shock at the jet base, **accelerating $e^{-/+}$ to > 200 TeV** ranges.
Now + LHAASO & HAWC results \rightarrow indication that UHE, VHE and HE φ may have distinct hadronic and leptonic origins : E & spatial resolution are key to understand this complex system

γ -ray astronomy community needs to continue observing microquasars!

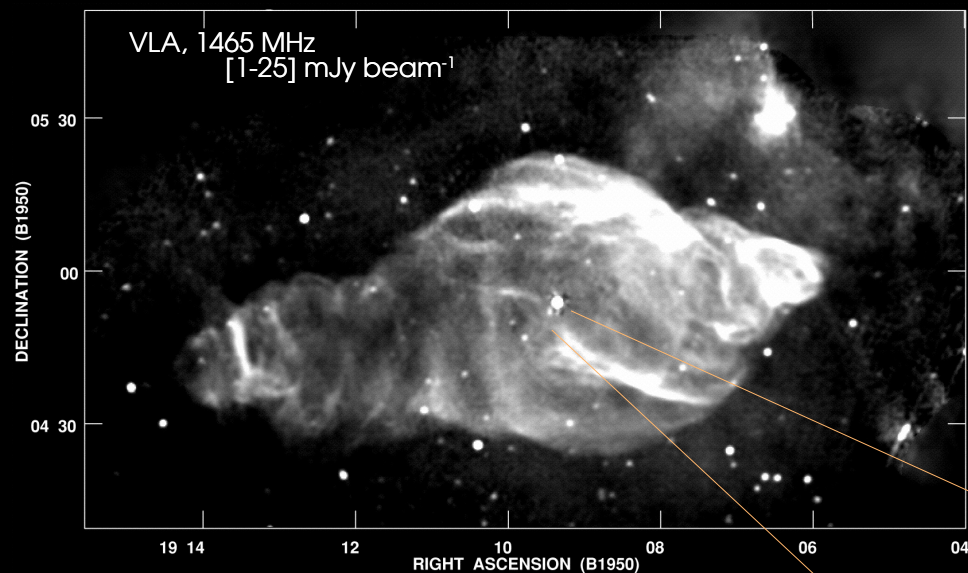
Why SS 433 (and this study) should be/remain on the MWL community's "radar"?

- Proof of concept → large-sized CT for bkg rejection
+ analysis optimisation to higher energy ranges
- **Spatially-resolved emission of jets in VHE?**
→ **IACTs** can provide tremendous info on
sites of VHE emission → **sites of particle acceleration/fresh injection**
→ *unparalleled observational evidence*
for **processes behind jets & their dynamics**
- Not all microquasars are thought to be HE nor VHE sources...
we may need to prove or disprove it!
Already a sample with claimed UHE emission, what about the Physics behind such?
Where are the acceleration sites?

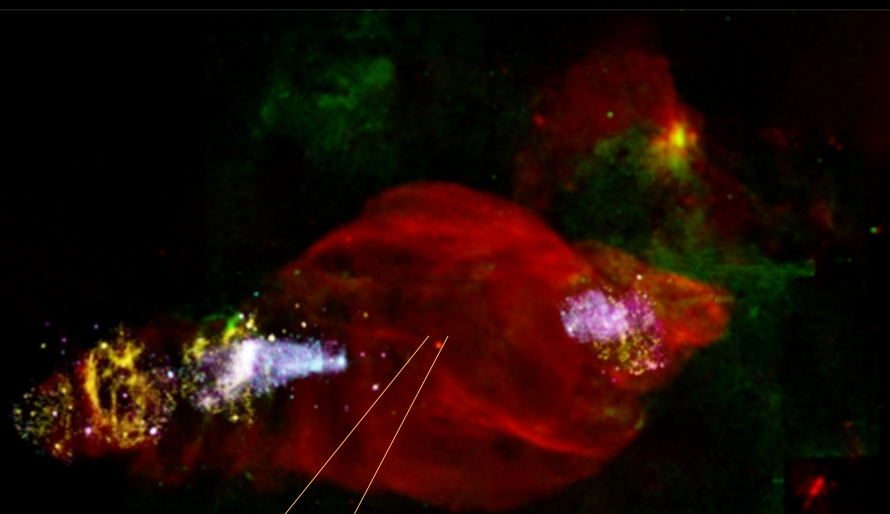
▶▶▶ **CTA** has the potential to change our landscape of
microquasars, binary systems and astrophysical jets ◀◀◀

Back-up

Radio/X-ray comparison



Dubner et al, 1998



Safi-Harb et al, 2022 + ref within

radio

optical

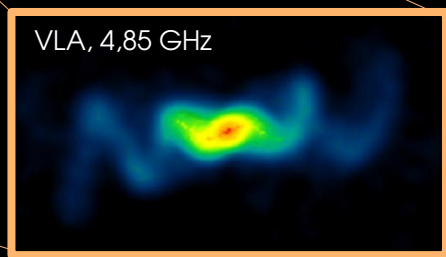
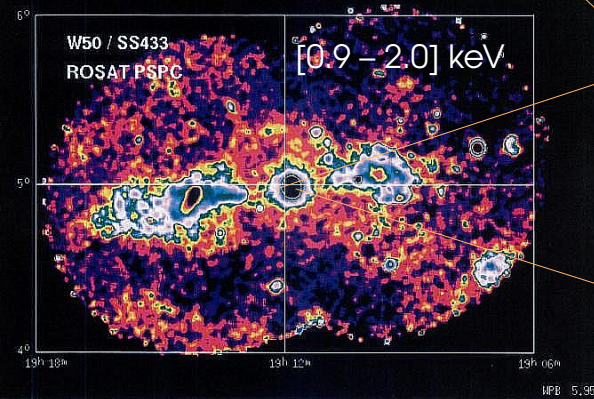
[0.5 – 1] keV

[1 – 2] keV

[2 -12 keV]

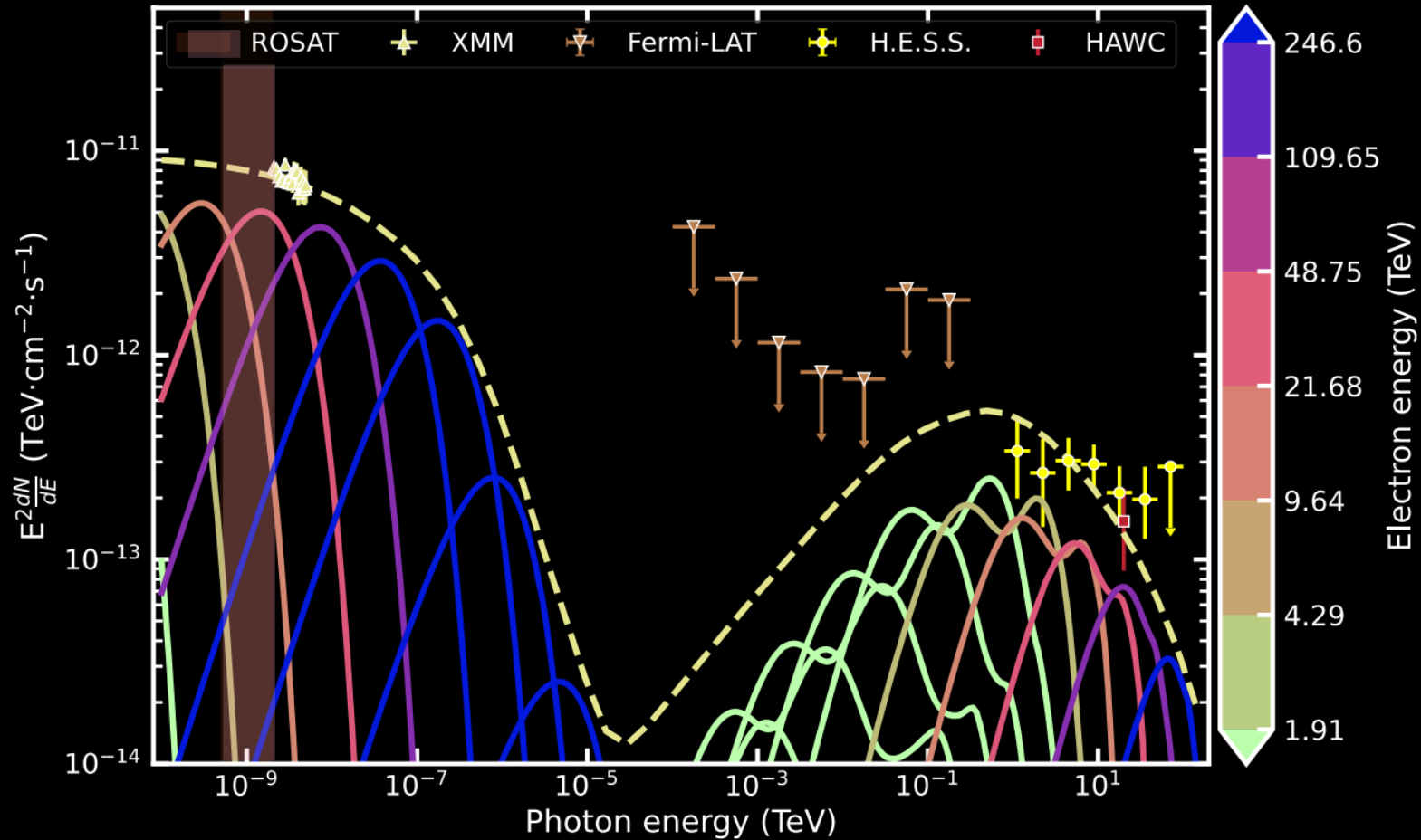
(X-ray : Newton-XMM & Chandra)

Brinkmann et al, 1996



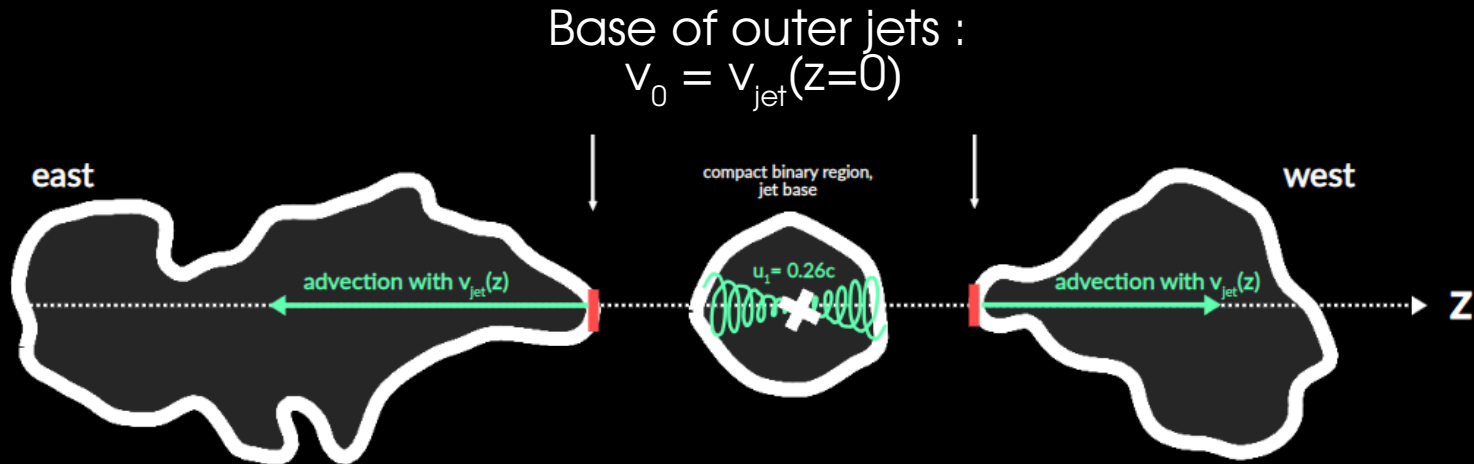
Blundell & Bowler, 2004

Electron populations for synchrotron and inverse-Compton components



One-dimensional advection-driven model

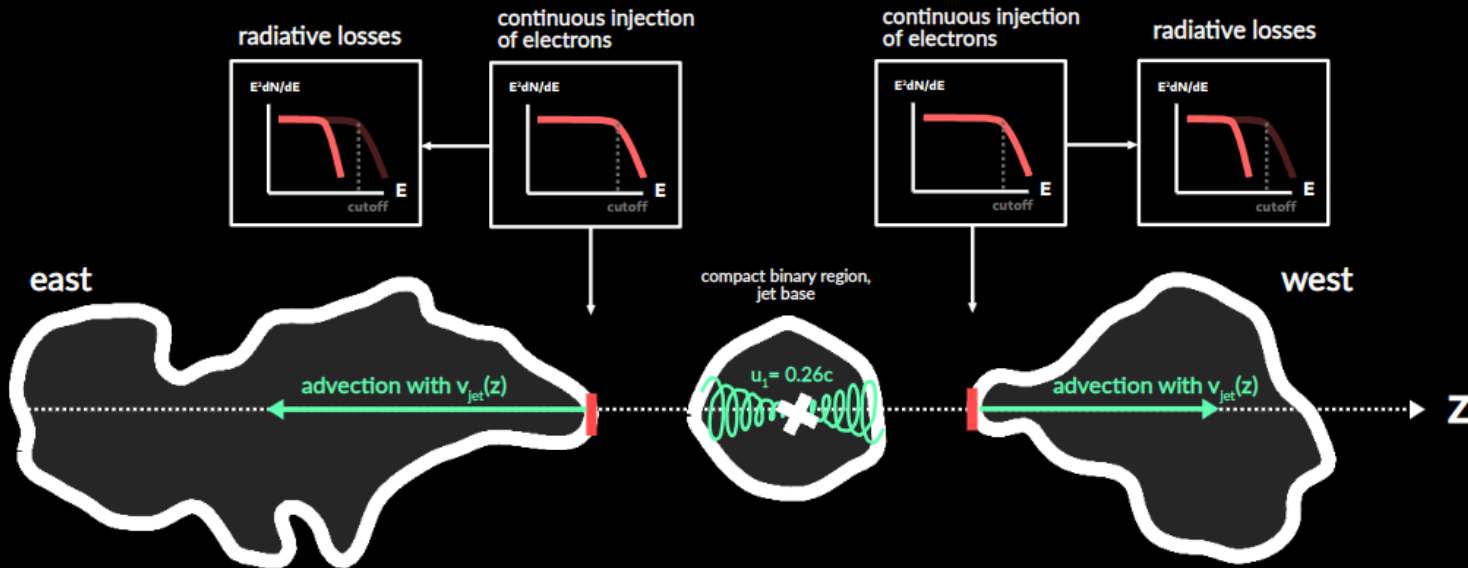
1D MC transport “simulation” along jet axis :



One-dimensional advection-driven model : fixed parameters

1D MC transport "simulation" along jet axis :

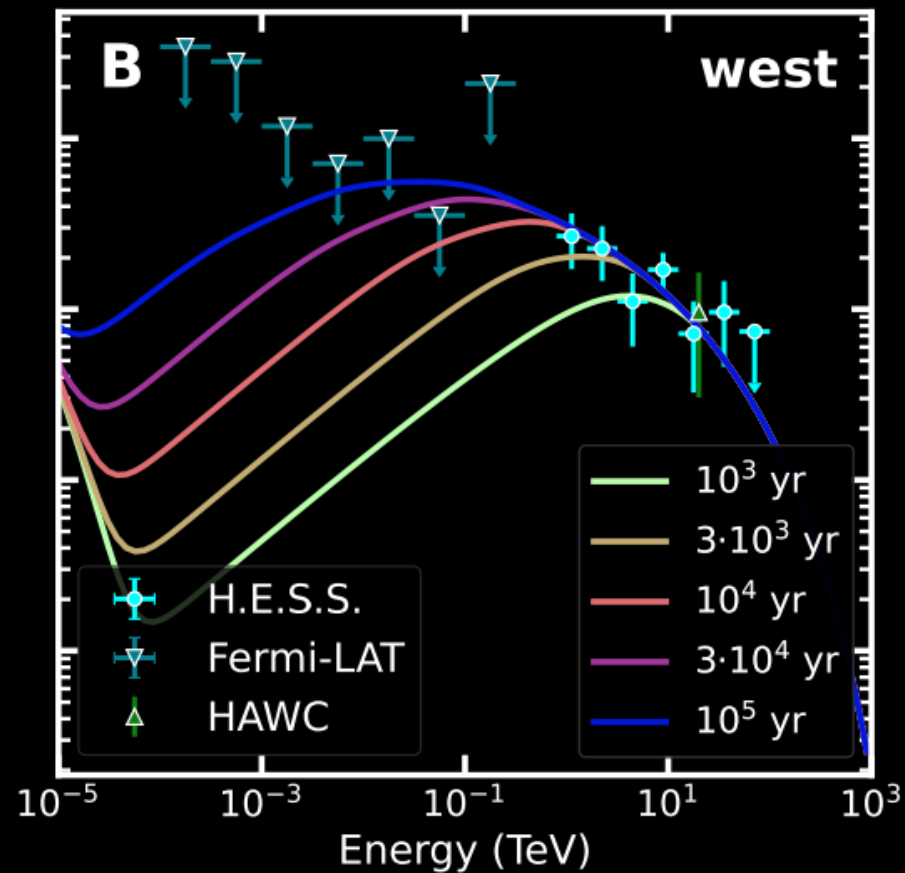
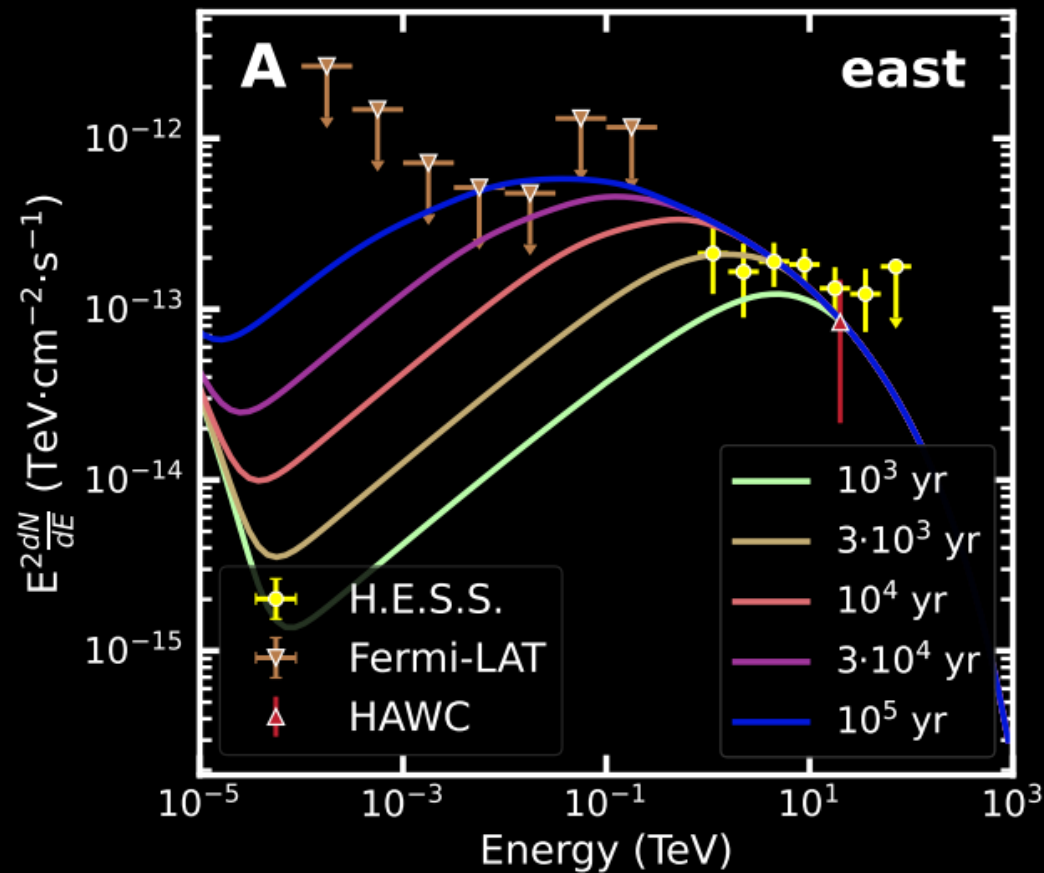
→ e^- spectrum, B : [fixed to best-fit MWL SED model]



➤ e^- injected
at $z = 0$
up to 10 kyr

➤ cooled

Injection duration spanning from [1 – 100] kyr



One-dimensional advection-driven model : fixed parameters

1D MC transport "simulation" along jet axis :

→ e^- spectrum, B : [fixed to best-fit MWL SED model]

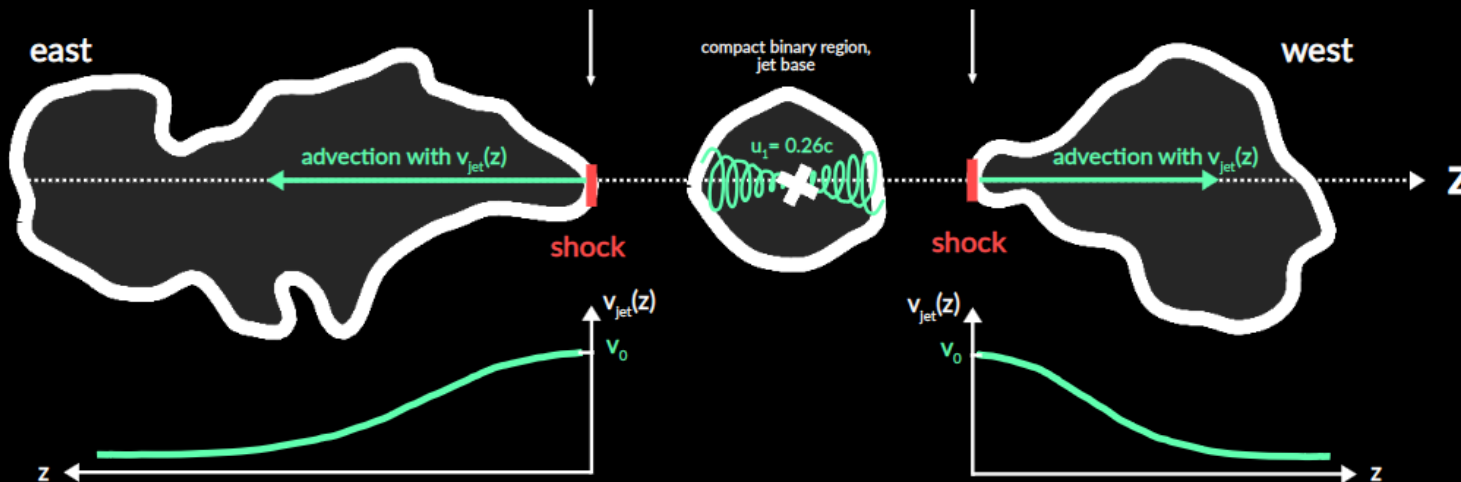
→ $v(z)$ [$= v_0 \Lambda(z)$]

➤ e^- injected
at $z = 0$
up to 10 kyr

➤ **advected by**
 $z_{\text{adv}} = v_{\text{jet}}(z) t$

➤ cooled

Base of outer jets :
 $v_0 = v_{\text{jet}}(z=0)$



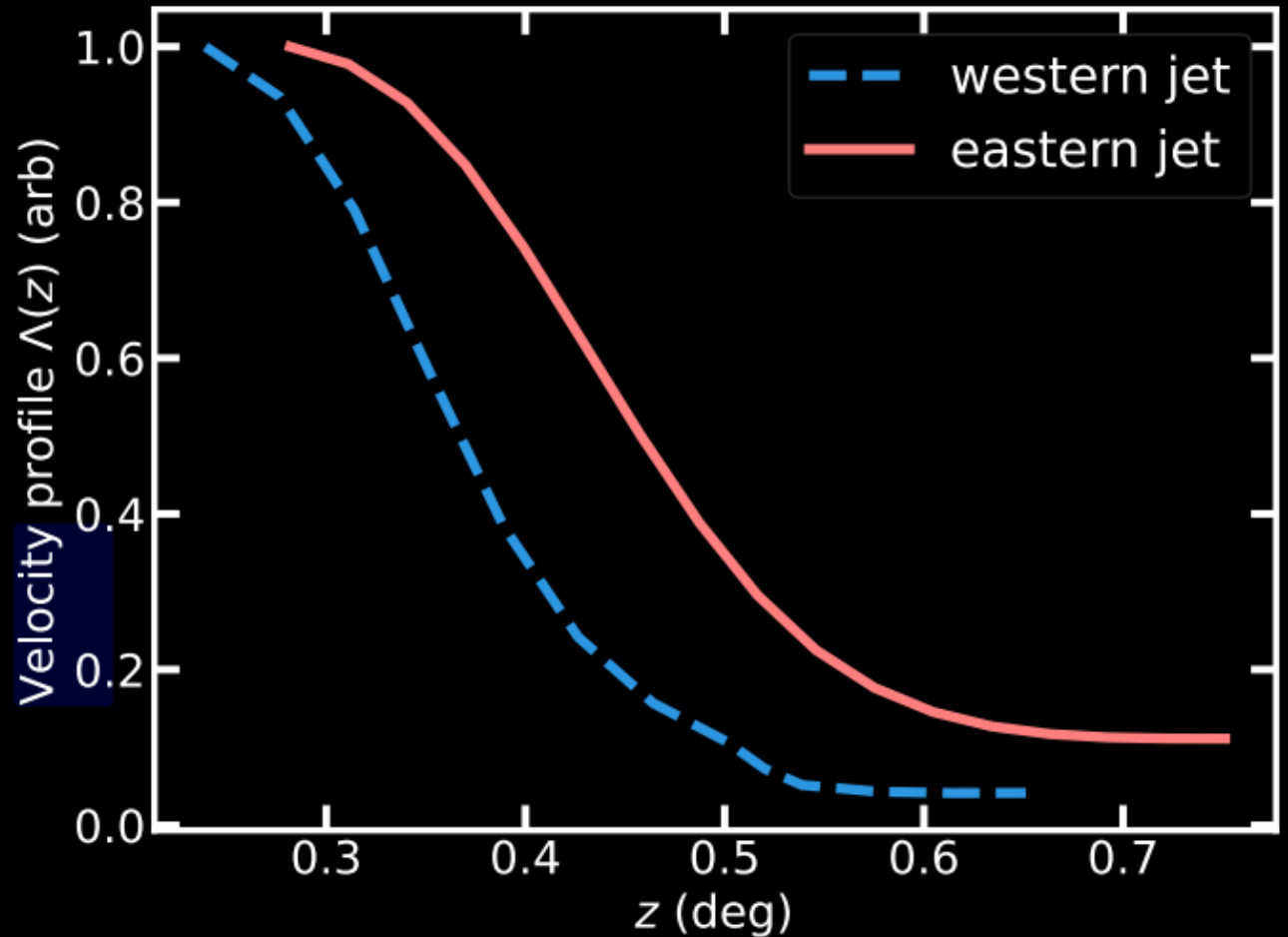
Decelerating jet

Derived

$$\Lambda = (\text{width}_{\text{jet, X-ray}})^{-2}$$

→ Evolution as
a function of z

Smoothed profile
to H.E.S.S. PSF size



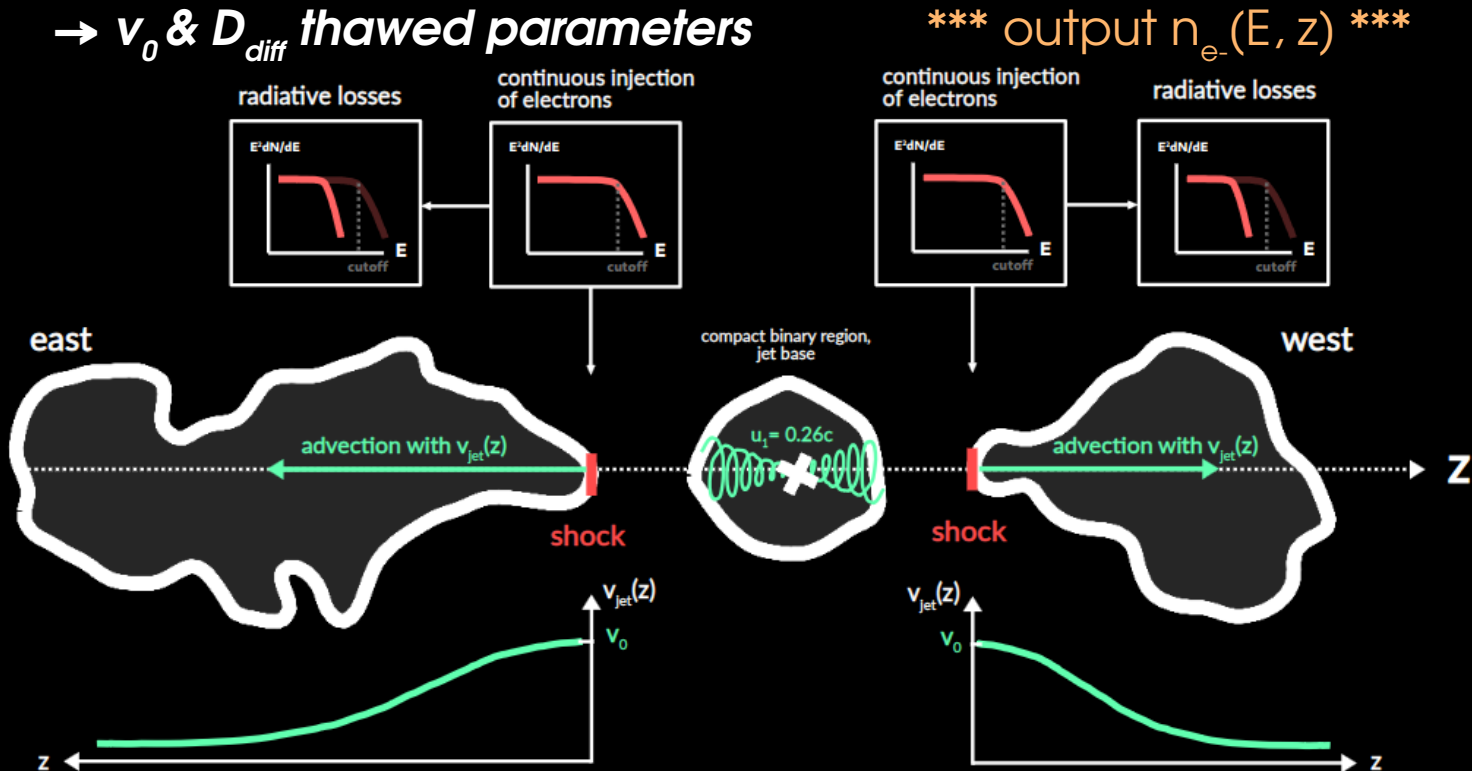
Inference of a strong shock at ~ 30 pc

1D MC transport "simulation" along jet axis :

→ e^- spectrum, B : [fixed to best-fit MWL SED model]

→ $v(z)$ [= $v_0 \wedge(z)$]

→ v_0 & D_{diff} *thawed parameters*



- e^- injected at $z=0$ up to 10 kyr
- advected by $z_{adv} = v_{jet}(z) \dagger$
- scaled with $r = (2 D_{diff} \dagger)^{1/2}$
- cooled

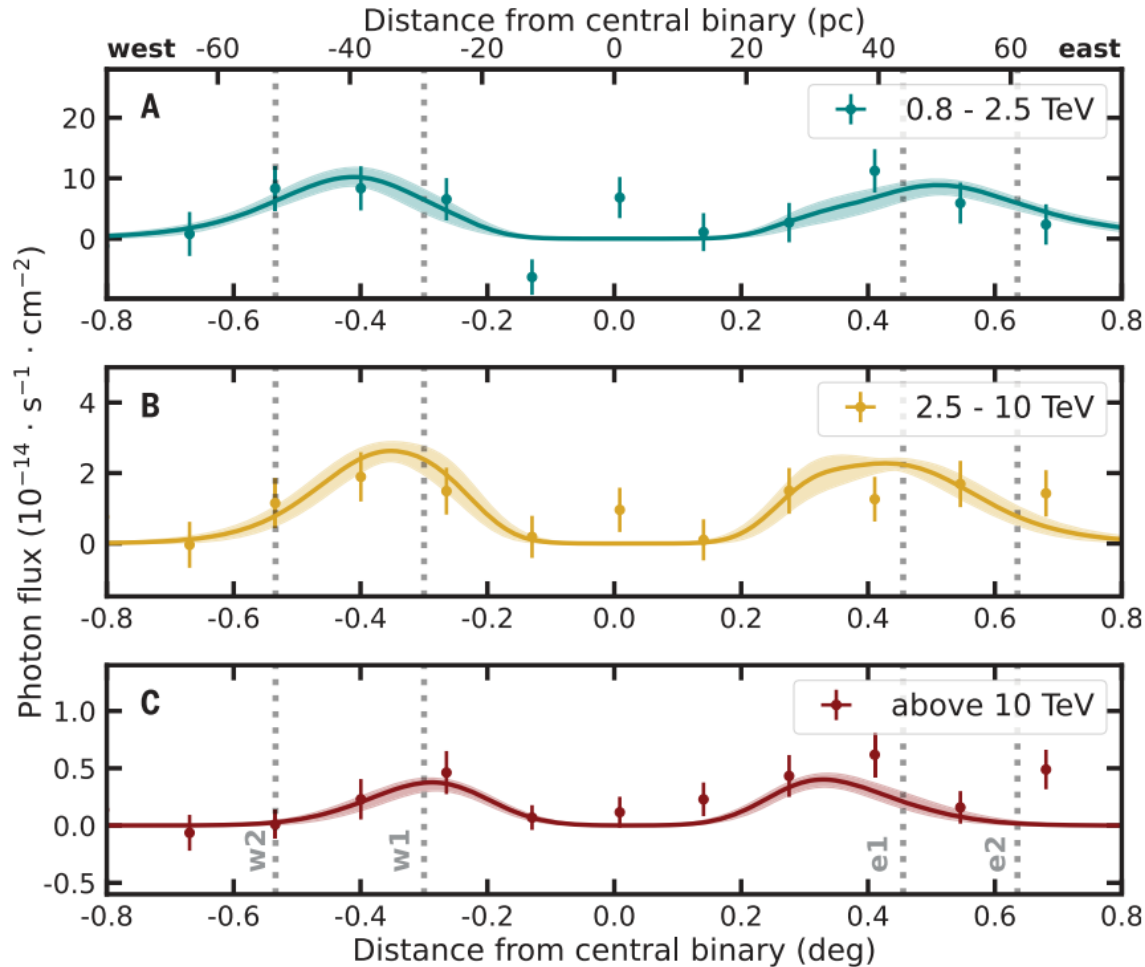
Shift of VHE peak towards the base of the outer jets : comparison model - data

- Solid lines :
→ Prediction from 1D "model" derived from computed $n_e(E, z)$

- Fit thawed parameters :

$$v_0 = v_{\text{jet}}(0)$$

$$D = D_{100} \left(\frac{E}{100 \text{ TeV}} \right)^{1/3}$$



Error bars :
→ statistical (at 1σ)
+ systematics

- Shaded :
combined stat uncertainty on the fit model parameters

Other jet velocity evolution cases

- Decelerating jet flow
- Constant velocity $\Lambda(z) = 1$:
 - \rightarrow constant section
w/o adiabatic loss
 - \rightarrow expanding section
with adiabatic loss

Best-fit (all consistent with $v_{\text{term}} \sim 0.023c$) :

$$v_0 = (0.083 \pm 0.026_{\text{stat}})c$$

$$D_{100} = (2.3 \pm 1.4) \cdot 10^{28} \text{ cm}^2 \text{ s}^{-1}$$

$$V_0 = (0.045 \pm 0.014_{\text{stat}})c$$

$$V_0 = (0.061 \pm 0.013_{\text{stat}})c$$

$$D_{100} = (4.7 \pm 4.1) \cdot 10^{27} \text{ cm}^2 \text{ s}^{-1}$$

Cannot distinguish between velocity evolution assumptions...

$$\text{Fit } D_{\text{diff}} < D_{\text{diff,Gal}}$$

But $v_0 \neq 0$

\rightarrow **advection** (+ radiative losses)

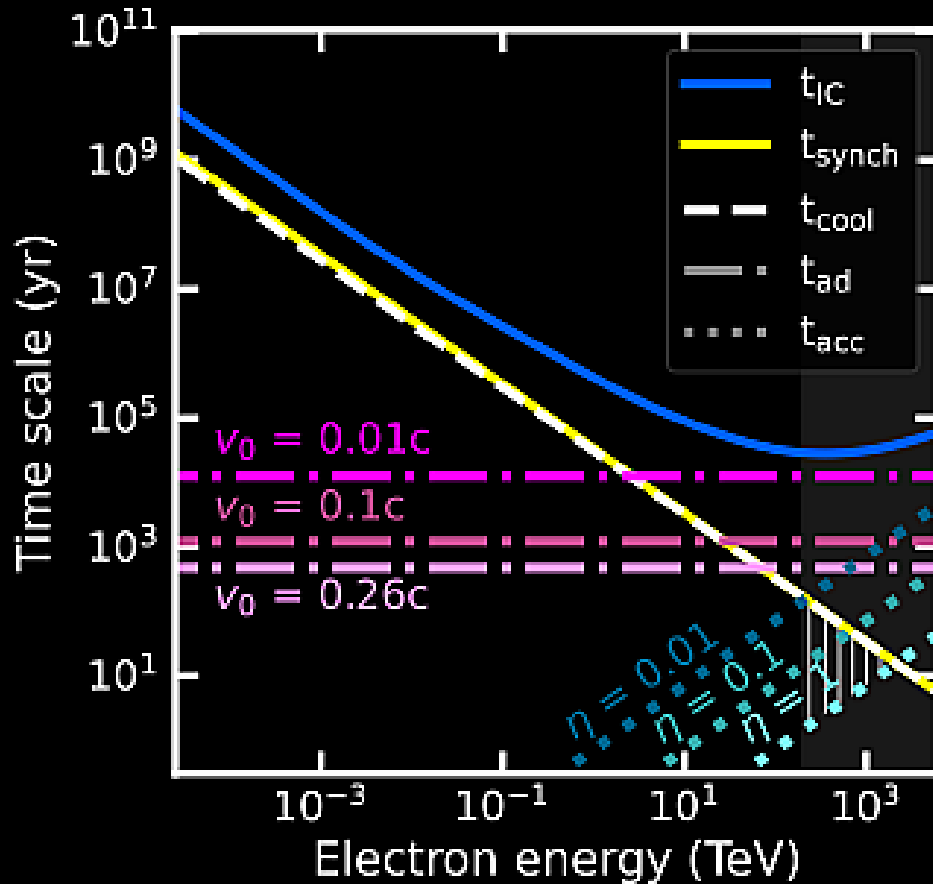
can explain

the shift of the VHE emission

along the jet axis

F
rom our study
H.E.S.S. Collaboration, 2024

Timescales



V_0 : velocity at the base of the outer jet

t_{ad} : adiabatic loss

$$t_{\text{acc}} = \frac{3}{u_1 - u_2} \left(\frac{D_1}{u_1} + \frac{D_2}{u_2} \right) \approx \frac{8 D_{\text{Bohm}}}{\eta u_1^2}$$

Assuming $u_1 = 0.26c$ (upstream)

$$\eta = \lambda_{e^-} / r_{g,e}$$

Greyish band : $E_{e^-, \text{max}} > 200 \text{ TeV}$

$$\eta (u_1 / 0.26c)^2 \gg 0.01$$

→ found $D_{\text{diff}} \ll t_{\text{cool}} v_0^2$

From our study
H.E.S.S. Collaboration, 2024

Contamination from the bright HESS J1908+063

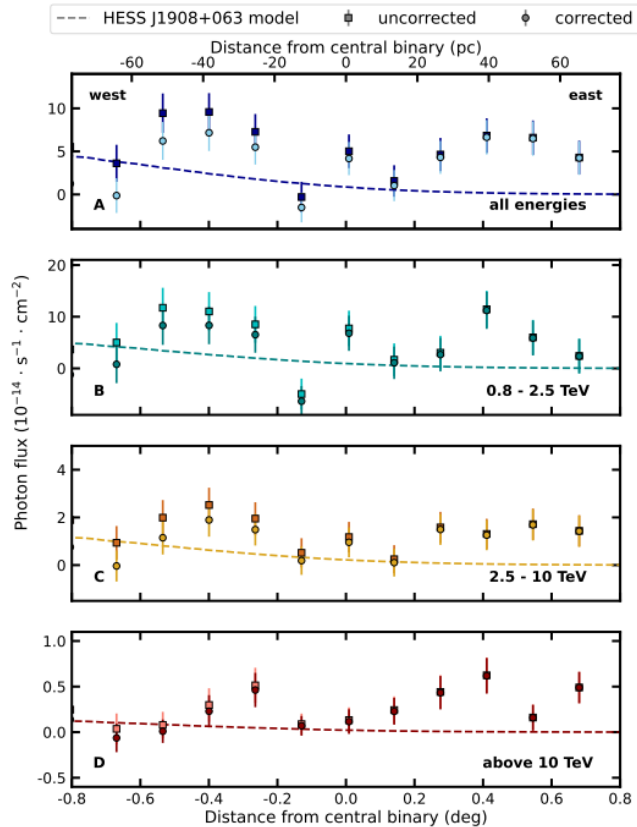


Figure S3: **Gamma-ray flux profiles along the jets showing the contamination of HESS J1908+063.** The data points represent the measured flux in spatial bins of 0.14° along the axis joining both jets through the central binary (Figure S2) for energies (A) above 0.8 TeV, (B) 0.8 to 2.5 TeV, (C) 2.5 to 10 TeV and (D) above 10 TeV. Squares and circles indicate the flux before and after subtracting HESS J1908+063. Error bars indicate the combined statistical (1σ) and systematic uncertainties. Circles in panels B-D are the same data as shown in Figure 4. The dashed lines show the flux of the HESS J1908+063 model at each location. The top axis assumes a distance to the system of 5.5 kpc (7).

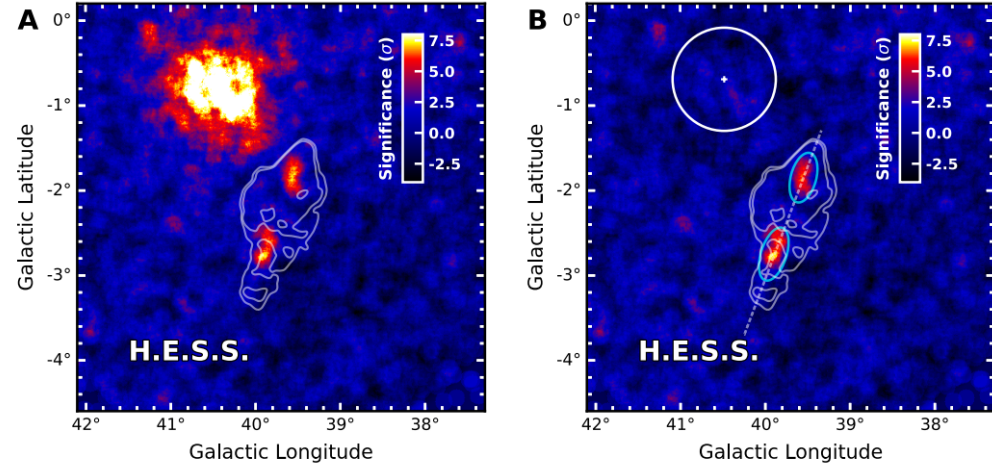
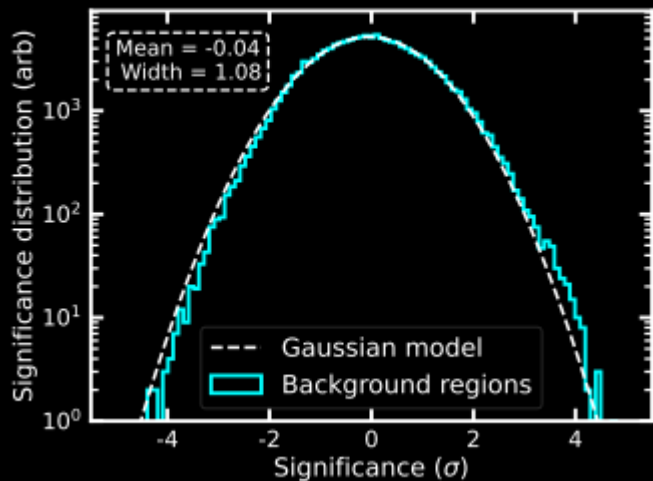


Figure S2: **Subtraction of HESS J1908+063.** Same as Figure 1A, but (A) before and (B) after subtracting the emission from the nearby extended source HESS J1908+063. In panel B, the white circle indicates the 68% containment region of the model fitted to HESS J1908+063, and the white cross is its best-fitting position. In both panels, the solid white contours show radio emission from the W 50 nebula (63–65). In panel B, the blue ellipses show the regions from where the spectral measurement of the jets is extracted (Figure 1B-C). The dashed line shows the axis across the jets used to derive the gamma-ray spatial profiles shown in Figures 4 and S3.

From our study
H.E.S.S. Collaboration, 2024

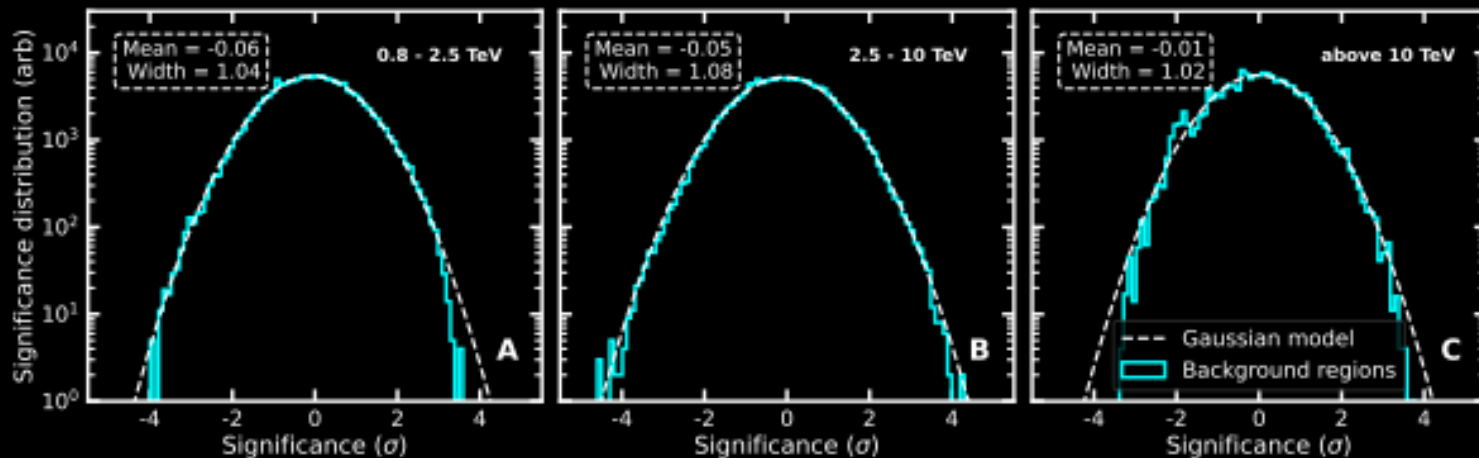
Background distribution



unbridged E range

From our study
H.E.S.S. Collaboration, 2024

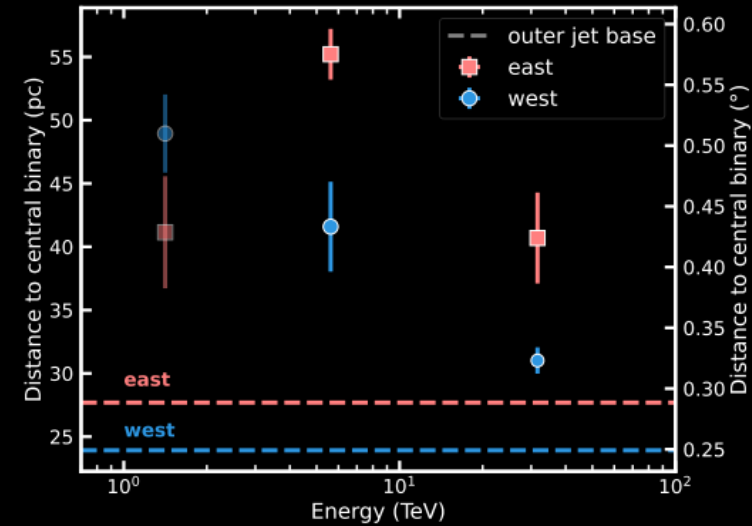
Energy bins



Morphology results, assuming $d = 5.5$ kpc

Best fit for G_{asym} , all E :

	unit	l	b	r_{maj}	r_{min}	θ
east	deg	39.875 ± 0.018	-2.687 ± 0.027	0.205 ± 0.035	0.044 ± 0.014	-19
	pc			19.68 ± 3.36	4.22 ± 1.35	
west	deg	39.564 ± 0.013	-1.853 ± 0.027	0.134 ± 0.036	0.046 ± 0.015	-19
	pc			12.86 ± 3.46	5.37 ± 1.44	



Best fit for G_{sym} , 3 E-bins :

side	energy (TeV)	l (deg)	b (deg)	r (deg)	$d_{\text{SS } 433}$ (deg)	$d_{\text{SS } 433}$ (pc)
east	0.8 to 2.5	39.913 ± 0.044	-2.614 ± 0.047	0.125 ± 0.022	0.428 ± 0.046	41.148 ± 4.424
	2.5 to 10	39.924 ± 0.018	-2.772 ± 0.021	0.085 ± 0.015	0.575 ± 0.021	55.212 ± 2.007
	above 10	39.840 ± 0.031	-2.643 ± 0.038	0.013 ± 0.029	0.424 ± 0.037	40.693 ± 3.593
west	0.8 to 2.5	39.537 ± 0.024	-1.759 ± 0.033	0.080 ± 0.016	0.510 ± 0.032	48.946 ± 3.089
	2.5 to 10	39.582 ± 0.024	-1.826 ± 0.037	0.095 ± 0.018	0.433 ± 0.037	41.590 ± 3.552
	above 10	39.560 ± 0.010	-1.951 ± 0.011	-	0.323 ± 0.011	31.015 ± 1.038

$> 5\sigma$: [2.5 – 10] TeV & > 10 TeV

--- : base (derived from X-rays)

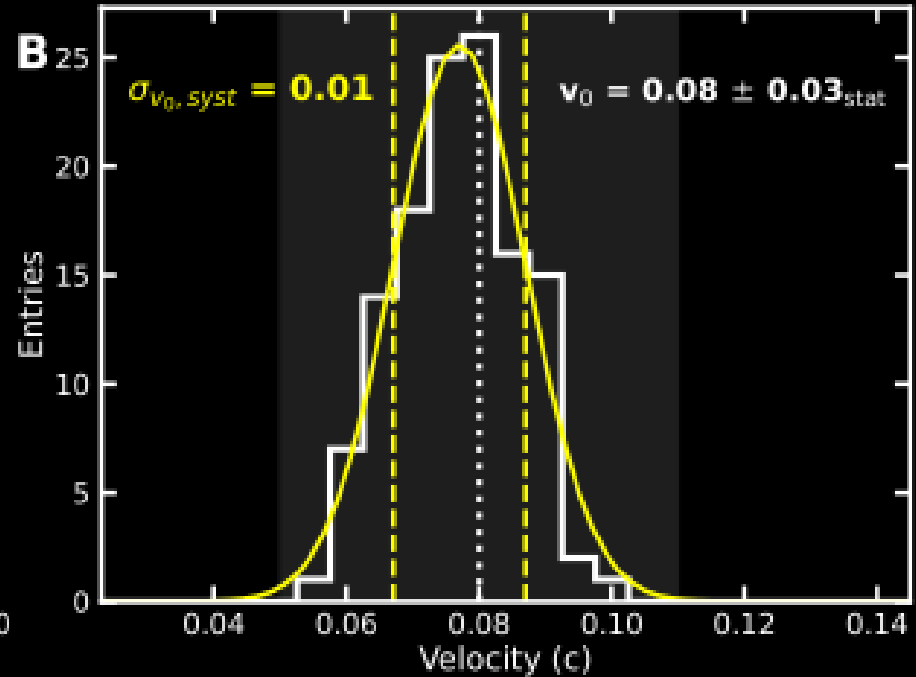
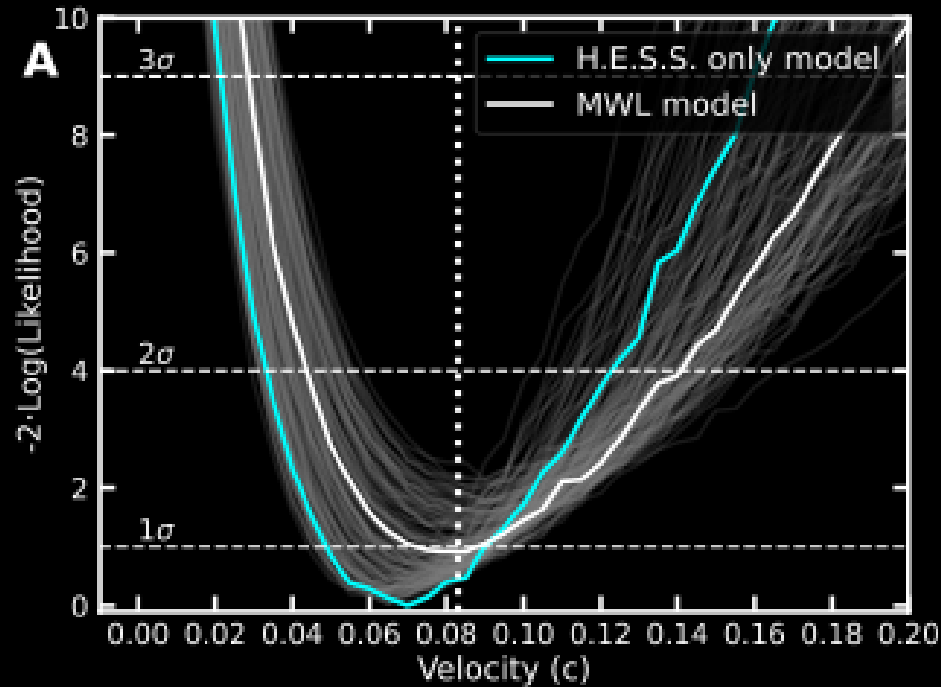
From our study
[H.E.S.S. Collaboration, 2024](#)

Systematics from model parameters

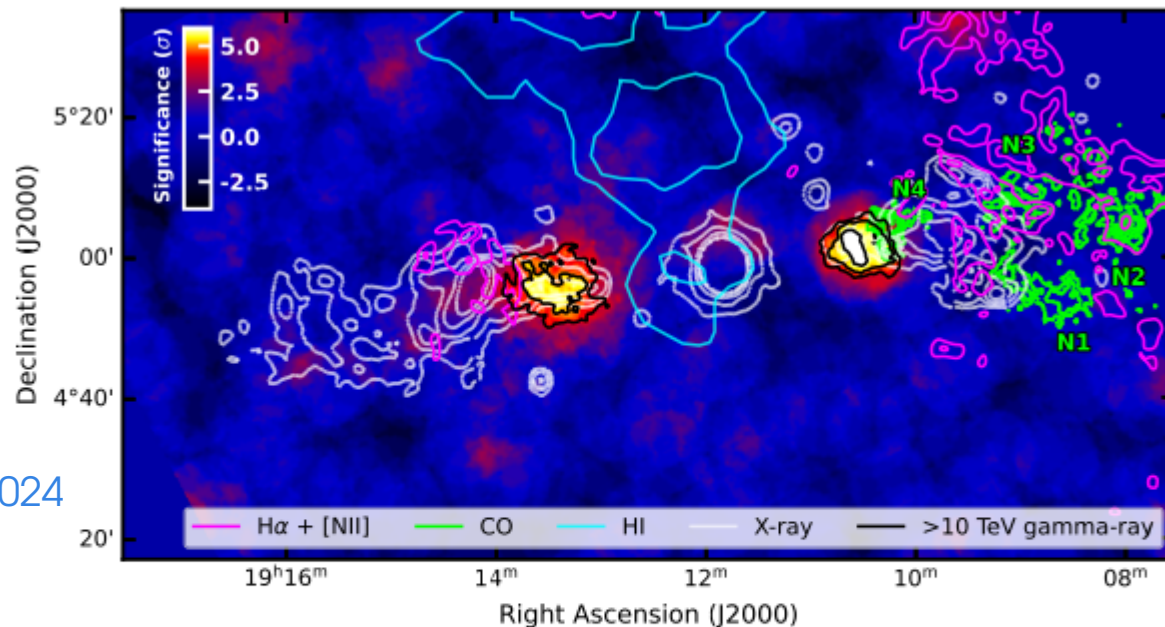
From our study

H.E.S.S. Collaboration, 2024

Combination of B and e- spectrum parameters
Initial v_0 systematics from MWL SED fit



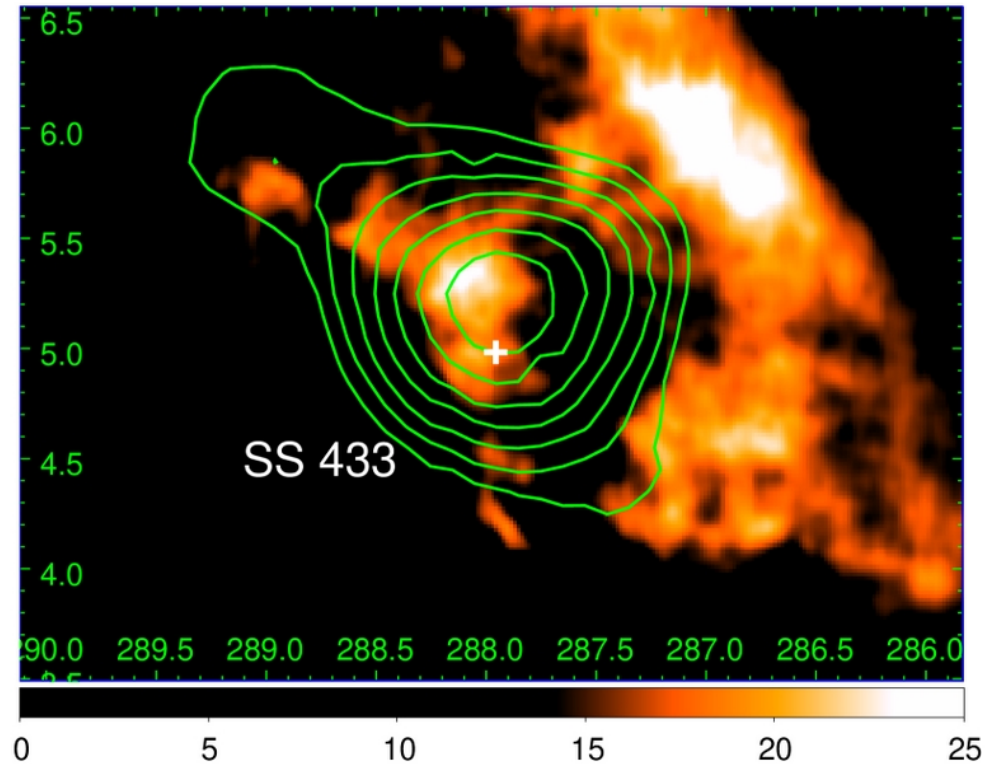
Material for hadronic processes (I)



From our study
H.E.S.S. Collaboration, 2024

Figure S16: Location of possible sites of hadronic interactions. The H.E.S.S. significance map above 10 TeV (rotated from the orientation in Figure 2C) compared to observed gas locations, which are possible target material for hadronic interactions. Equatorial coordinates are shown for the J2000 equinox. Black contours indicate significances of 4, 5 and 6 σ in the H.E.S.S. map. The pink contour indicates H α + [NII] emission from ionised gas (83), green corresponds to CO observations revealing four molecular clouds N1 to N4 (82) and light blue to neutral hydrogen emission from diffuse neutral gas (79). The ROSAT X-ray contours (14) are shown for reference in white. There is no correlation between any of the potential targets and the H.E.S.S. emission above 10 TeV.

Material for hadronic processes (II)



From
LHAASO collaboration, 2024

Extended Data Figure 1: Map of the H I emission observed with Arecibo integrated in the interval 65–82 km s⁻¹[25]. The green contours show the gamma-ray emission above 100 TeV from 3σ with a step of 1σ. The image has been scaled by $\sin |b|$ (b is Galactic latitude) to enhance the features far from the Galactic plane[59]. The horizontal and vertical axes are R.A. and decl. in J2000.